

Optimization of Stochastic Parallel Gradient Descent Algorithm via Power Spectrum Method

Yang Song^{1,2}, Tao Chen¹, Jianli Wang¹ and Bing Qiao¹

¹ Changchun Institute of Optics, Fine Mechanics and Physics, Chinese Academy of Sciences, No.3888 South-East Lake Road, Changchun, 130033, China

² Department of Mechatronic Engineering, University of Chinese Academy of Sciences, No.19A Yuquan Road, Beijing, 100049, China

Received: 3 Jul. 2015, Revised: 2 Sep. 2015, Accepted: 3 Sep. 2015

Published online: 1 Jan. 2016

Abstract: A method is proposed to optimized the adaptive optics (AO) system based on the stochastic parallel gradient descent (SPGD) algorithm. In order to increase the speed of convergence, we use the power spectrum method. First of all, we analysis the relation between the atmosphere turbulence power spectrum which can be described as Von Karman spectrum and the stochastic perturbation, and then, we optimize the cutoff frequency of the Von Karman spectrum based on the dependency of the two item mentioned before, finally, an AO model based on the SPGD algorithm is set up, and the phase aberration with the Von Karman spectrum is simulated numerically. Results show that, compared with the conventional SPGD algorithm, the method proposed in this paper not only has a great advantage in increasing the convergence speed, but also can improve the performance index. Experiment proves the correction of the theory and the feasibility of the method. The method proposed in this paper will give a great instruction to the real time AO system.

Keywords: adaptive optics, power spectrum, stochastic parallel gradient descent algorithm, convergence speed

1 Introduction

Due to the complicated atmospheric structure and the changeable motion state, the optical beam generates turbulence effects in the atmospheric transmission, such as the intensity fluctuation, beam expansion, and wave-front aberration and so on, which seriously affect the quality of the light wave transmission. The basic principles of the traditional adaptive optical system are to use the wave-front sensor to detect the information of the aberration wave-front and to compensate the aberration by controlling the wave-front corrector. The wave-front aberrations brought by the strong scintillation during the transmission path and the fluctuation arisen from receiving the amplitude at the receive plane are the main causes of the conventional adaptive optics (AO) systems detective error.

Although, the adaptive optics technique based on the wave-front detection has been widely used in the fields of astro observation, laser transmission and beam control and so on [1], the conventional adaptive optical system will not work when the wave-front cannot be measured directly, for example, the atmospheric turbulence is

relatively strong, the wave-front distorts [2,3], or the multiphoton microscopy is used for imaging in Biology [4,5,6].

Compared with the conventional AO systems, the adaptive optics without a wave-front sensor doesn't require wave-front detecting, reforming, therefore, it has the advantages of simple structure; being unrestricted by aberration conditions such as the scintillation, strong adaptability to the complicated environment, etc., which, has gradually become the hotspot in research in recent years [7,8,9]. There are some algorithms have been commonly used in the control algorithm of the adaptive system at present, including the stochastic parallel gradient descent (SPGD) [10,11], genetic algorithm(GA) [12], and simulated annealing(SA) [13,14]. Stochastic parallel gradient descent (SPGD) algorithm is one of the most useful control algorithms used in model free systems, with the advantages of simple implementation, parallel computing of all control parameters, and suitable for real-time applications, etc. however, the disadvantage of slow convergence speed for the traditional SPGD algorithm is becoming more and more prominent, along

* Corresponding author e-mail: songyang2661@sina.com

with the increase of the correction unit in the adaptive optics.

Research shows that, the convergence speed of SPGD algorithm has positive correlation with the phase perturbation caused by the random disturbance voltage and the wave-front aberration to be corrected [10, 15].

In order to describe the physical characteristics and rules of the atmospheric turbulence, a mathematical model based on the atmospheric turbulence shall be established. Von Karman spectrum, as a relatively typical spectral model used to describe the turbulence, has the advantage of small difference between the phase structure function and the experimental data, therefore, the power spectrum method can be used to produce the phase perturbation of atmospheric turbulences which accords with Von Karman spectrum and the random disturbance voltage in the algorithm to improve the statistical correlation between the wave-front aberration to be corrected and the phase perturbation caused by the random disturbance voltage, so as to achieve the purpose to increase the convergence speed for the traditional SPGD algorithm.

In this paper, SPGD optimization algorithm based on the power spectrum method is proposed, the training set is produced by using the numerical simulation method, and the algorithm parameter is determined on the basis of the training set; and then the simulation model of adaptive optics is built up to analyze the impact of methods proposed in this paper on the convergence property of the adaptive optics.

2 SPGD algorithm and its convergence speed

The basic idea of SPGD algorithm: during the N th iteration, the performance metric of the system $J[U^{(n)}]$ is obtained by applying the correction voltage vector $U^{(n)} = \{U_1^{(n)}, \dots, U_j^{(n)}, \dots, U_N^{(n)}\}$ to each N control channels of the deformable mirror; in the $(n+1)$ th iteration, firstly, a set of perturbation voltage vector $\Delta U = \{\Delta U_1, \dots, \Delta U_j, \dots, \Delta U_N\}$ is generated randomly; secondly, the system performance metric $J(U^+)$ is obtained by applying voltage vector $U^+ = U^{(n)} + \Delta U$ to the deformable mirror; and finally, the system performance metric $J(U^-)$ is obtained by applying the voltage vector $U^- = U^{(n)} - \Delta U$ to the deformable mirror, and the variation of the system performance metric ΔJ is as follows:

$$\Delta J = J(U^+) - J(U^-) \quad (1)$$

The correction voltage vector applied to the deformable mirror after $n+1$ iterations is:

$$U^{(n+1)} = U^{(n)} + \gamma \Delta U \Delta J \quad (2)$$

Each component ΔU_j in the random disturbance voltage ΔU is subordinated to the Bernoulli distribution and independent of one another, namely, the value of

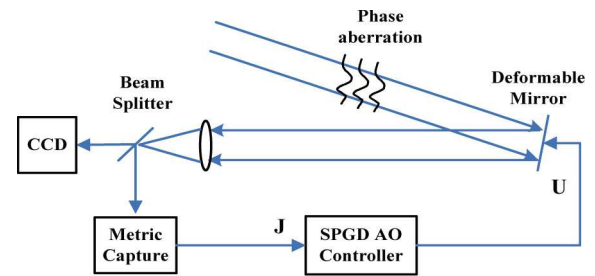


Fig. 1: Numerical simulated model of AO system.

amplitude of each component is fixed and the probabilities of each value (negative and positive) are equal: $\Delta U_j = \sigma$, $\Pr[\Delta U_j = \pm\sigma] = 0.5$. In the formula, γ is a gain coefficient, whose symbol can be determined by the optimized direction of the performance metric function. Take a negative number when the optimized direction is the minimal value of the performance metric function, and take positive number on the contrary. Optimize the system performance metric by multiple closed-loop iterative method in order to correct the wave-front phase aberration.

Adaptive optics simulation model based on SPGD algorithm is as shown in Figure 1. SPGD algorithm is used to control the deformable mirror to correct the phase aberration caused by the atmospheric turbulence, while the Root Mean Square (RMS) is adopted to measure the system performance metric.

According to formula (2), as a gradient estimation, $\gamma \Delta U \Delta J$ has a great influence on the convergence speed of the algorithm. When the amplitude of the random disturbance voltage σ and the gain coefficient γ are fixed, the value size of the gradient term $\gamma \Delta U \Delta J$ is proportional to that of the absolute value $|\Delta J|$, the closer the $|\Delta J|$ to the actual gradient is, the faster the convergence speed of the algorithm is. Therefore, the convergence speed can be quickened by narrowing the gap between $|\Delta J|$ and the actual gradient. $\delta m(x, y)$ is supposed to be the phase distortion caused by the random perturbations voltage, while $\phi(x, y)$ is supposed to be the wave-front phase aberration, the minimum gap between $|\Delta J|$ and the actual gradient can be realized only when $\delta m(x, y)$ and $\phi(x, y)$ have the greatest statistical correlation [15]. Actually, if each iteration $\delta m(x, y)$ has a perfect correlation with $\phi(x, y)$, the residual voltage obtained from wave-front detection is almost equivalent to the random disturbance voltage applied to the corrector, namely the two have the same correction speed.

However, when applying the random phase perturbation which accords to the Bernoulli distribution, the statistics different homology between the random phase perturbation and the wave-front aberrations to be corrected determines that it is hard to improve the convergence speed of traditional SPGD algorithm constitutionally. Therefore, increasing the statistical correlation

between $\delta m(x,y)$ and $\phi(x,y)$ can improve the convergence property of the algorithm.

3 The basic deduction

According to the working principle of the deformable mirror, the wave-front phase $\delta m(x,y)$ generated by the random perturbations can be described linearly with the response functions of the DM actuators:

$$\delta m(x,y) = \sum_{j=1}^N \Delta U_j S_j(x,y) \tag{3}$$

In the formula, the perturbation voltage applied to the j th actuator in the deformable mirror is ΔU_j , the deformation response function $S_j(x,y)$ is as shown in formula (4), the actuator number of the deformable mirror is N [16].

$$S_j(x,y) = \exp \left[\ln \omega \left(\frac{\sqrt{(x-x_j)^2 + (y-y_j)^2}}{d} \right)^\alpha \right] \tag{4}$$

In formula (4), ω is a coupling value of the driver, (x_i, y_i) is a position coordinate of the i th driver, α is a Gaussian function index, and d is a separation distance between adjacent drivers. The coupling value refers to the ratio of the center coordinate's deformation of adjacent drivers and the center coordinate's maximum deformation of adjacent drivers. In this paper, the separation distance of the deformable mirror driver d is 14 mm, the Gaussian function index α is 2.4, while the coupling value of the driver ω is 10.8% [16].

In the form of power spectrum, $\delta m(x,y)$ can be expressed as:

$$\delta m(x,y) = C \sum_{k_x} \sum_{k_y} R(k_x, k_y) \sqrt{F_\Phi(k_x, k_y)} \exp[j(k_x x + k_y y)] \Delta k_x \Delta k_y \tag{5}$$

In the formula, $x = m\Delta x$, $y = n\Delta y$, m, n are integers, and $\Delta x, \Delta y$ are sample intervals in the airspace; $k_x = m'\Delta k_x$, $k_y = n'\Delta k_y$, m', n' are integers, and $\Delta k_x, \Delta k_y$ are sample intervals in the wave count area; the constant C is used to adjust the phase screen parameters from the scaling factor $(\Delta k_x \Delta k_y)^{1/2}$; $R(k_x, k_y)$ is a Gaussian number that meet the zero-mean and the unit variance; and $F_\Phi(k_x, k_y)$ is used to describe the power spectrum model of the turbulence [17]. The commonly-used typical spectrum models mainly include Kolmogorov spectrum, Tatarskii spectrum, exponential spectrum, Von Karman spectrum and corrected Von Karman spectrum, among which, Von Karman spectrum is the correction of Kolmogorov spectrum and Tatarskii spectrum, in addition, the experimental results show that the data of Von Karman spectrum is closer to the experimental data than that of the exponential spectrum when transferring in the collimated laser beam [18]. In order to contain the internal and external scales of turbulence into the

turbulence spectrum, Von Karman spectrum has been further modified. In this paper, Von Karman spectrum used can be expressed as:

$$F_\Phi(k) = 0.033 C_n^2 \exp(-k^2/k_m^2) (k^2 + k_0^2)^{-11/6} \tag{6}$$

In the formula, C_n^2 is a refractive-index structure constant in the atmosphere, $k_m = 5.92/l_0$, l_0 and L_0 respectively are the inner scale and outer scale of the turbulence, while $k_0 = 2\pi/L_0$ is a corresponding spatial wave number of L_0 [19]. According to the formulas (3)~(6), the phase perturbation distribution of the random disturbance voltage ΔU_j calculated by the power spectrum can be obtained:

$$\Delta U_j = \frac{C \sum_{k_x} \sum_{k_y} R(k_x, k_y) \sqrt{0.033 C_n^2 \exp(-k^2/k_m^2) (k^2 + k_0^2)^{-11/6}} \exp[j(k_x x + k_y y)] \Delta k_x \Delta k_y}{\exp \left[\ln \omega \left(\frac{\sqrt{(x-x_j)^2 + (y-y_j)^2}}{d} \right)^\alpha \right]} \tag{7}$$

Similarly, if the phase aberration $\phi(x,y)$ caused by the atmospheric turbulence is described by the power spectrum method, $\phi(x,y)$ and $\delta m(x,y)$ generated from the formula (7) have a certain statistical correlation, which can improve the convergence speed of the algorithm.

It can be seen from the formula (7) that, the computational complexity of the random voltage vector is codetermined by the phase perturbation distribution generated by the power spectrum inversion $\delta m(x,y)$ and the response function of the deformable mirror $S_j(x,y)$. For example, the calculated amount is big when the phase screen sample interval in formula (5) is $\Delta k_x = \Delta k_y = 256$; the calculated amount will be even bigger if the actuator number of the deformable mirror N is bigger, namely, its computational efficiency will reduce significantly as the actuator number increases. To simplify the calculated amount and to increase the calculation speed, compare the value generated when the wave-front phase aberration $\phi(x,y)$ is applied to the j th actuator of the deformable mirror with the mean value generated when the phase aberration is applied inside caliber of the deformable mirror, if the difference value is bigger than 0, a negative value shall be taken for the random disturbance voltage, and a positive value shall be taken on the contrary, which not only guarantee the correlation between $\delta m(x,y)$ and $\phi(x,y)$, but also improve the calculation speed. Please see formula (8) for the empirical formula.

$$U_j = \begin{cases} -1; & \phi(x-x_j, y-y_j) - \bar{\phi}(x,y) > 0 \\ +1; & \phi(x-x_j, y-y_j) - \bar{\phi}(x,y) \leq 0 \end{cases} \tag{8}$$

In the formula, $\phi(x,y)$ presents the wave-front phase aberration, $\bar{\phi}(x,y) = \frac{1}{S} \int \phi(x,y) dx dy$ presents the mean value of the wave-front phase aberration inside the caliber of the deformable mirror.

According to the conclusion of the reference 20, when the performance metric function is $J = \frac{1}{S} \int \Phi^2(x,y) dx dy$,

we get

$$\langle \delta J \rangle \leq \langle \delta J \rangle_{\max} = P^2 + \frac{2}{s} \max_{\delta(x,y)} \left| \int \langle \delta m(x,y) \Phi(x,y) \rangle dx dy \right|.$$

In the formula, P is a constant far less than 1, and $\frac{1}{s} \int \langle \delta m^2(x,y) \rangle dx dy \leq P^2$, $\Phi(x,y) = \phi(x,y) - \delta m(x,y)$ are residual phases. It can be obtained from the formula that, the maximum expectation value of the performance index $\langle \delta J \rangle_{\max}$ depends on the crosscorrelation coefficient of the residual phase $\Phi(x,y)$ and the wave-front phase perturbation caused by the random voltage $\delta m(x,y)$, the bigger the value of the crosscorrelation coefficient is, the bigger the value of $\langle \delta J \rangle$ is.

In order to verify the correlation between the wave-front phase perturbation $\delta m(x,y)$ caused by the random voltage generated by the formula (8) and the wave-front aberration $\phi(x,y)$ caused by the atmospheric turbulence, the cross-correlation function $\eta(x,y)$ of $\delta m(x,y)$ and $\phi(x,y)$ is introduced hereinafter:

$$\eta(x,y) = \frac{E[(\delta m(x,y) - \overline{\delta m(x,y)}) (\phi(x,y) - \overline{\phi(x,y)})]}{\sqrt{E(\delta m(x,y) - \overline{\delta m(x,y)})^2} \sqrt{E(\phi(x,y) - \overline{\phi(x,y)})^2}} \quad (9)$$

Substitute the formula (8) into the formula (3) to calculate the value of η , the bigger the value is, the better the correlation between $\delta m(x,y)$ and $\phi(x,y)$ is.

4 The analysis of simulation results

When the structure constant of atmospheric turbulence C_n^2 is fixed, in different observation systems, the wave-front of incident light wave can be considered as the plane wave and the spherical wave based on the circumstances [21]. Taking the plane wave as an example, the relationship between the atmospheric coherent length r_0 and the altitude distribution of C_n^2 is:

$$r_0 = \left[0.432k^2 \int_0^L C_n^2(h) dh \right]^{-0.3} \quad (10)$$

By substituting the formula (10) into the formula (6), we can get the correlation between the power spectral density that accords with the atmospheric turbulence and the atmospheric coherent length as follow:

$$F_{\Phi}(f_x, f_y) = 0.49r_0^{-5/3} (f_x^2 + f_y^2 + f_0^2)^{-11/6} \quad (11)$$

In the computer simulation, discretize the formula (11) to get the following formula:

$$F_{\Phi}(k'_x, k'_y) = 0.49r_0^{-5/3} ((m'\Delta f_x)^2 + (n'\Delta f_y)^2 + f_0^2)^{-11/6} \quad (12)$$

In the formula, $-M/2 \leq m' \leq M/2 - 1$, $-N/2 \leq n' \leq N/2 - 1$, (M, N) , and $(\Delta f_x, \Delta f_y)$ respectively are sampling points and sampling frequencies of the phase screen [22].

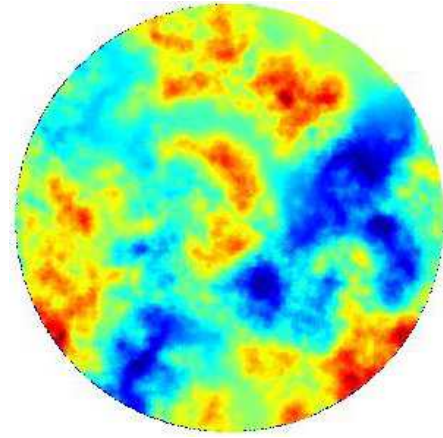


Fig. 2: Phase aberration with the von karman spectrum.

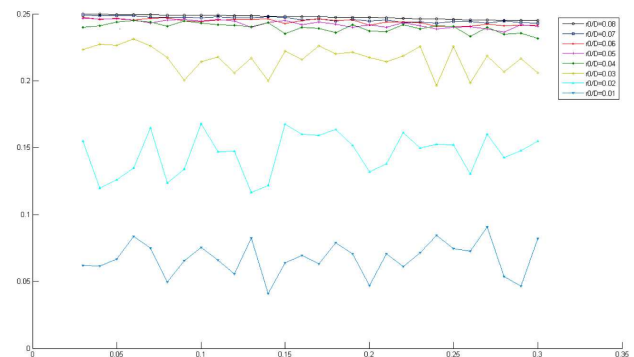


Fig. 3: Trend of η along with f_0 before optimization.

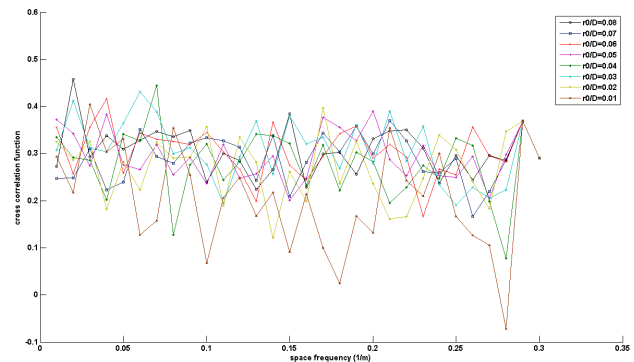


Fig. 4: Trend of η along with f_0 after optimization.

Remove the tip and tilt component, make the ratio between the wave-front caliber D and the atmospheric coherent length r_0 be $\frac{D}{r_0} = 10$; when the spatial frequency f_0 is 0.01 m^{-1} , we can get the wave-front aberration following the Von Karman spectrum by using the power spectrum method, as shown in Figure 2.

Research shows that, the value of the atmospheric coherent length r_0 get bigger as the observed altitude

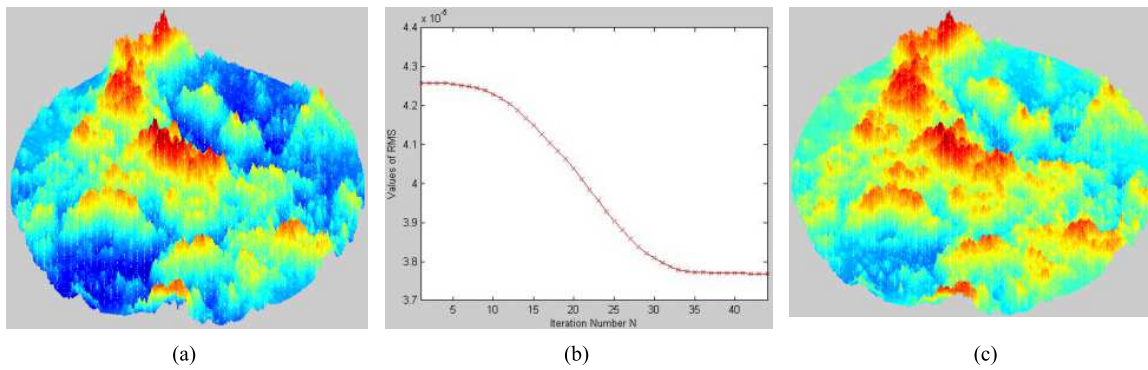


Fig. 5: (a) Initial phase aberration; (b) Trend of RMS before optimization; (c) Phase aberration before optimization.

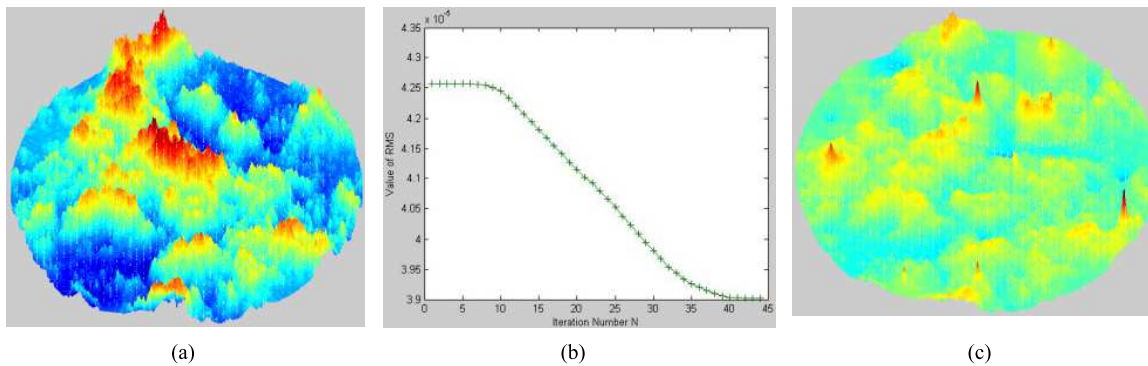


Fig. 6: (a) Initial phase aberration; (b) Trend of RMS after optimization; (c) Phase aberration after optimization.

increases, ranging from a few centimeters to tens of meters [22]. Based on the near-earth observation, simulation analysis is carried out to the incident wave-front aberrations by selecting different r_0 values ranging from 0.01~0.08 m to get the changing curve for the cross-correlation coefficient η of $m(x,y)$ and $\phi(x,y)$ under the different space frequency f_0 before and after the optimization, as shown in Figures 3 and 4:

The conclusions obtained from Figure 3: (1) the correlation difference between $\delta m(x,y)$ and $\phi(x,y)$ is big when the atmospheric coherent length r_0 is different; the correlation difference of the algorithm is smaller when r_0 changes within 0.04~0.08 m; the correlation difference of the algorithm is smaller while r_0 is getting smaller when r_0 is less than 0.04 m. (2) the correlation curve changes irregularly as the spatial frequency f_0 varies when the atmospheric coherent length r_0 is the same.

The conclusions obtained from Figure 4: (1) the correlation between $\delta m(x,y)$ and $\phi(x,y)$ is different when the atmospheric coherent length r_0 is different, and the whole fluctuation range is not big, namely, the impact on the correlation of the algorithm is small when r_0 changes within 0.01~0.08 m; (2) the correlation curve changes irregularly as the spatial frequency f_0 varies when the atmospheric coherent length r_0 keeps the same. It can be

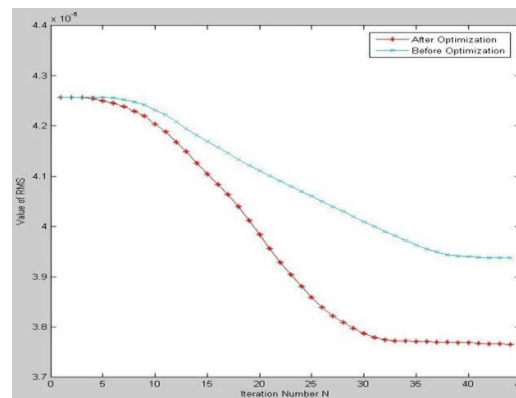


Fig. 7: Trend of RMS along with iterations.

seen from the figure that, the value of the cross-correlation curve is significantly smaller than the value of r_0 for other values when $r_0 = 0.01$ m, that is to say, the impact on the correlation of the algorithm is big when the atmospheric turbulence is severe and the atmospheric coherent length $r_0 \leq 0.01$ m.

By the comparison of Figure 3 and Figure 4, we found, the algorithm presents the irregular variations as the spatial frequency f_0 varies both before and after the

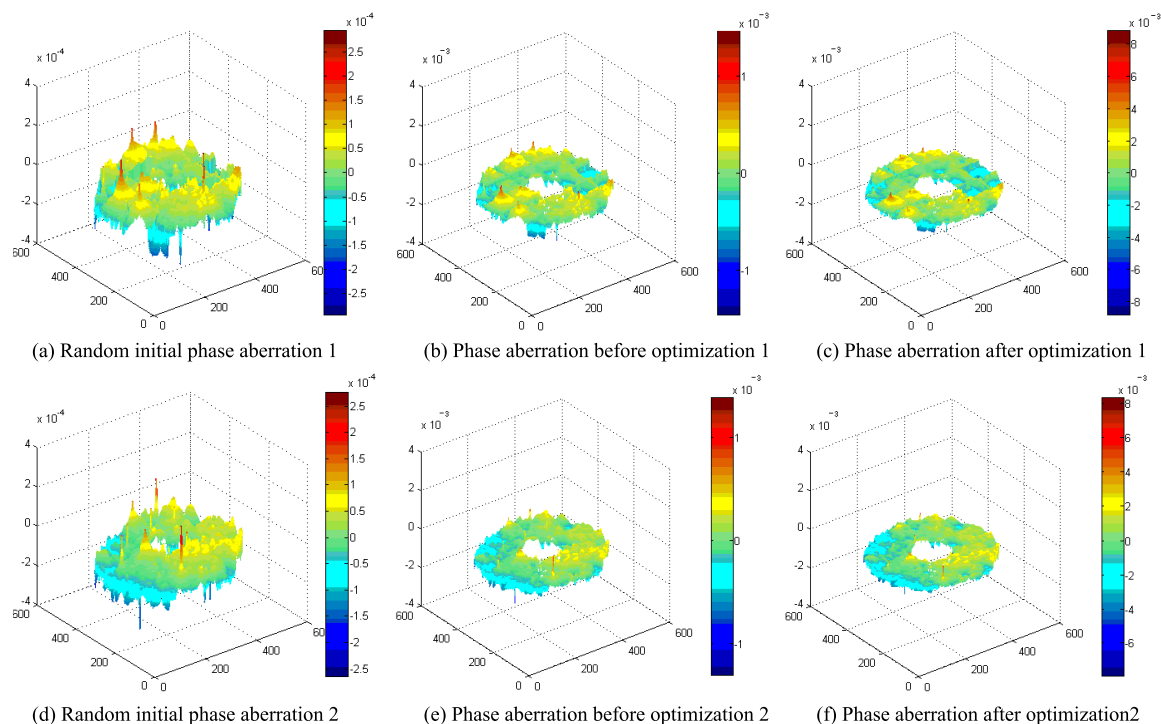


Fig. 8: The results of different Initial phase aberration.

optimization; after the optimization, the impact of the atmospheric coherent length r_0 on the correlation of the algorithm is smaller, the range of application is wider, and the correlation of the algorithm is improved about 17% compared with that before the optimization (the mean value before the optimization is about 0.25, and the one after is about 0.3).

With the combination of the above conclusions, we select any spatial frequency value randomly: when $r_0 = 0.6 \text{ m}$ and $f_0 = 0.19 \text{ m}^{-1}$, the voltage value of the random disturbance is obtained by substituting $f_0 = 0.19 \text{ m}^{-1}$ into the formula (8).

The wave-front aberration is generated by using the power spectrum method, and the below results are achieved by adopting SPGD algorithm before and after the optimization to optimize the same distorted wave-front respectively:

Figure 5 shows the correction capability of the algorithm before optimization: (a) shows the phase aberration before correction, (b) and (c) respectively show the curves of performance metric change and the wave-front aberration through 45 iterations before optimization; Figure 6 shows the correction capability of the algorithm after optimization: (a) represents wave-front aberration same as that in Figure 5, (b) and (c) respectively represent the curves of performance metric change and the wave-front aberration through 45 iterations after optimization. By the comparison of the

Figure 5(c) and Figure 6(c), we can get that, the correction capability to the wave-front aberration is stronger after the optimization when the initial phase aberrations are the same.

In order to quantitatively measure the increase of the convergence speed, the following trend of RMS along with iterations is obtained by comparing Figure 5 (b) with Figure 6 (b). Details are as shown in Figure 7.

Analyzing Figure 7 from the y-coordinate, when RMS value of the initial distorted wave-front is 4.26×10^{-4} and the traditional SPGD algorithm has passed through 45 iterations, the wave-front RMS value 3.9×10^{-4} tends to a standstill, but RMS value can be reduced to around 3.78×10^{-4} by applying the optimization algorithm mentioned in this paper; from the x-coordinate, the SPGD algorithm before optimization tends to converge after 37 iterations, however, the convergence can be reached after 30 iterations by using the optimization algorithm proposed in this paper.

In order to verify the reliability of the algorithm, we optimize the different initial phase aberration generated randomly by using SPGD algorithm before and after the optimization respectively, and get the following results as shown in Figure 8:

It can be seen from the above analysis that, improving the correlation between the phase aberration of wave-front to be corrected and the phase perturbation caused by the random voltage can effectively increase the

convergence speed and the correction capability of the algorithm, and analysis result of the performance index based on the SPGD algorithm verifies the feasibility to optimize the random perturbation voltage to improve the convergence speed and the correction capability of the algorithm. Therefore, to effectively improve the convergence properties and the performance index of the algorithm, we can select the right power spectrum to generate the corresponding perturbation voltage according to the statistical property of the phase aberration.

5 Conclusion

In this paper, a method to optimize the SPGD algorithm by using the power spectrum method is proposed, the statistical homology of the wave-front distortion to be corrected and the random perturbation voltage is improved and the convergence speed of SPGD algorithm in the adaptive optics is increased by optimizing the random perturbation voltage. The numerical simulation model based on this method is established, and the convergence speed and the correction capability of SPGD algorithm under different atmospheric coherent lengths before and after the optimization are simulated. In addition, simulation results show that, optimizing the disturbed voltage can improve the convergence speed of SPGD algorithm to a great extent.

On the other hand, the method proposed in this paper is not limited to the Von Karman spectrum, the model built based on the different practical situations and the characteristics of atmospheric turbulence obtained previously can provide better guidance to the practical engineering.

It will be the focus in the further work how to apply the algorithm proposed in this paper in the engineering test.

References

- [1] Hardy JH. Adaptive optics for astronomical telescopes. New York: Oxford University Press; 1991.
- [2] Primmermen CA, Price TR, Humphreys RA, et al. Atmospheric-compensation experiments in strong-scintillation conditions. *Appl Opt* 1995;34(2):2081-8.
- [3] Baranova NB, Mamaev AV, Pilipetsky NF, et al. Wave-front dislocations: topological limitations for adaptive systems with phase conjugation. *J Opt Soc Am A* 1983;73(5),pp.525-8.
- [4] Marsh P, Burns D, Girkin J. Practical implementation of adaptive optics in multiphoton microscopy. *Opt Express* 2003;11(10),pp.1123-30.
- [5] Xi P, Andegeko Y, Pestov D, et al. Two-photon imaging using adaptive phase compensated ultrashort laser pulses. *J Biomed Opt* 2009;14(1),pp.014002-7.
- [6] Poland SP, Wright AJ, Girkin JM. Evaluation of fitness parameters used in an iterative approach to aberration correction in optical sectioning microscopy. *Appl Opt* 2008;47(6),pp.731-6.
- [7] Jia Jianlu, Wang Jianli, Zhao Jinyu, et al. Optimization of adaptive optical wave-front algorithm[J]. *Opt. Precision Eng*, 201321(4),pp.1026-1031
- [8] Yang Huizhen, Chen Bo, Li Xinyang, et al. Experimental demonstration of stochastic parallel gradient descent control algorithm for adaptive optics system[J]. *Acta Optica Sinica*, 2008, 28(2), pp.205-210
- [9] Chen Bo, Yang Huizhen, Zhang Jinbao, et al. Performance index and convergence speed of parallel gradient descent algorithm in adaptive optics of point source[J]. *Acta Optica Sinica*,2009,29(5), pp.1143-1148
- [10] M. A. Vorontsov, G.W. Carhart. Adaptive Optics Based On Analog Parallel Stochastic Optimization: Analysis And Experimental Demonstration[J]. *J. Opt. Soc. Am. A*, 2000, 17(8), pp.1440-V1453.
- [11] Yang Huizhen, Li Xinyang, et al. Restoration of turbulence-degraded extended object using the stochastic parallel gradient descent algorithm: numerical simulation[J]. *Opt Express* 2009; 17(5), pp.3052-62.
- [12] Mukai R, Wilson K, Vilnrotter V. Application of genetic and gradient descent algorithms to wave-front compensation for the deep-space optical communications receiver[R/OL]. Pasadena: Jet Propulsion Laboratory, 2005. http://tmo.jpl.nasa.gov/progress_report/42-161/161U.pdf.
- [13] Zommer S, Ribak E N, Lipson S G, et al. Simulated annealing in ocular adaptive optics [J]. *Opt Lett*, 2006, 31(7), pp. 1-3.
- [14] El-Agmy R, Bulte H, Greenaway A H, et al. Adaptive beam profile control using a simulated annealing algorithm [J]. *Opt Express*, 2005, 13(16), pp. 6085-6091.
- [15] Chen Bo, Li Xinyang, Jiang Wenhan. Optimization of Stochastic Parallel Gradient Descent Algorithm for Adaptive Optics in Atmospheric Turbulence [J]. *CHINESE JOURNAL OF LASERS*, 2010, 37(4), pp.959-964.
- [16] DING Xinzhi GUAN Chunlin. The finite element method simulation of the deformable mirror's influence function [J]. *OPTICAL INSTRUMENTS*, 2008, 30(1), pp.40-44.
- [17] ZHANG Huimin LI Xinyang. Numerical simulation of wavefront phase screen distorted by atmospheric turbulence [J]. *Opto-Electronic Engineering*, 2006, 33(1), pp.14-19.
- [18] Luo Chenghu. Study of laser transmission characteristics of atmospheric turbulence and the effect on the SAL [D]. 2012.
- [19] Larry C. Andrews, Ronald L. Phillips. *Laser Beam Propagation through Random Media [M]*. Second Edition. Washington: SPIE, 2005, pp.782.
- [20] M. A. Vorontsov, V. P. Sivokon. Stochastic parallel-gradient-descent technique for high-resolution wave-front phase-distortion correction [J]. *J. Opt. Soc. Am. A*, 1998, 15(10), pp.2745-2758.
- [21] ZHANG Xiao-fang, YU Xin, YAN Ji-xiang. Influence of atmospheric turbulence on image resolution of optical sensing system [J]. *OPTICAL TECHNIQUE*, 2005, 31(2), pp.263-265.
- [22] Yang Lianchen, Shen Mangzuo, Guo Yong hong. The Speckle Imaging Simulation Of Space Objects [J]. *ACTA PHOTONICA SINICA*, 2000, 29(12), pp.1108-1112.



Yang Song is studying for her PhD degree in Mechatronic Engineering at University of Chinese Academy of Sciences. Her research interest is in the area of adaptive optics technology.



Jianli Wang is Professor of Mechatronic Engineering at University of Chinese Academy of Sciences. His research interest is in the area of General technology of high resolution ground-based telescope.



Tao Chen is Professor of Mechatronic Engineering at University of Chinese Academy of Sciences. He mainly engaged in the research of photoelectric precision tracking and measuring technology.



Qiao Bing is deputy senior engineer of Changchun Institute of Optics, Fine Mechanics and Physics, Chinese Academy of Sciences, she mainly engaged in the research of electronic design.